

# Facile Assembly of Ni–Co Hydroxide Nanoflakes on Carbon Nanotube Network with Highly Electrochemical Capacitive Performance

Hongyuan Chen,<sup>†,‡</sup> Feng Cai,<sup>†,‡,§</sup> Yiran Kang,<sup>†,‡,||</sup> Sha Zeng,<sup>†,‡,⊥</sup> Minghai Chen,<sup>\*,†,‡</sup> and Qingwen Li<sup>\*,†,‡</sup>

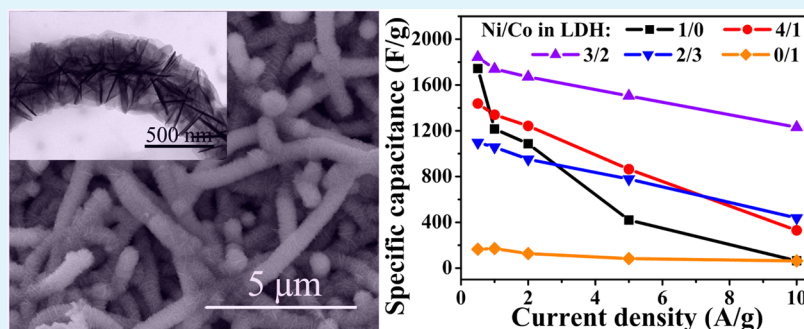
<sup>†</sup>Suzhou Institute of Nano-Tech and Nano-Bionics and <sup>‡</sup>Key Lab of Nanodevices and Applications, Suzhou Institute of Nano-Tech and Nano-Bionics, Chinese Academy of Sciences, Suzhou 215123, P. R. China

<sup>§</sup>Nano Science and Technology Institute, University of Science and Technology of China, Suzhou 215123, P. R. China

<sup>||</sup>School of Materials Science and Engineering, Zhengzhou University, Zhengzhou 450001, P. R. China

<sup>⊥</sup>University of Chinese Academy of Sciences, Beijing 100049, P. R. China

## Supporting Information



**ABSTRACT:** Herein, we demonstrate the high-density assembly of Ni–Co hydroxide nanoflakes on conductive carbon nanotube (CNT) network through a simple and rapid chemical precipitation method, presenting a low-cost and high-performance scaffold for pseudosupercapacitor. It is found that the Ni–Co layered double hydroxide (LDH) nanoflakes prefer to proliferate around large-diameter CNTs (diameter > 50 nm), with conductive CNT network well-maintained. Such hierarchical nanostructures show greatly improved specific surface areas compared with bare CNT network and are freestanding without other organic binder, which can be directly employed as a binder-free compact electrode assembly. By optimizing the chemical composition of as-precipitated LDH nanoflakes, the resultant  $\text{Co}_{0.4}\text{Ni}_{0.6}(\text{OH})_2$  LDH/CNT composite nanostructures exhibit the largest specific electrochemical capacitance and the best rate performance, with their capacitance up to 1843 F/g under a low current density of 0.5 A/g and maintained at 1231 F/g when the current density is increased 20 times to 10 A/g. Importantly, such hierarchical nanostructures tend to prevent the electrode from severe structural damage and capacity loss during hundreds of charge/discharge under a high rate (2 A/g), ensuring the electrode with high-energy density (51 W h/kg) at power density of 3.3 kW/kg.

**KEYWORDS:** hierarchical nanowire, layered double hydroxide, nanoflake, carbon nanotube paper, supercapacitor

## INTRODUCTION

Fast development prolongation of electric vehicles and portable electronic devices have greatly inspired the fundamental research and technology development for energy storage devices with high capacity, high energy/power density, and long-term performance stability.<sup>1</sup> Among numerous electrochemical power sources, electrochemical capacitor, also being called supercapacitor, is a competitive alternative due to its advantages in energy storage applications, such as high power densities, long cyclic lifetime, high safety, and low price.<sup>2</sup> Various porous carbon materials with high specific areas have been designed and synthesized as electrodes for high-performance supercapacitors based on electrochemical double-layer capacitance.<sup>3</sup> However, poor energy density is their

common drawback for practical applications. To ensure the supercapacitors with excellent specific capacitance and energy density, pseudocapacitive materials, such as conductive polymers,<sup>4</sup> transition metal oxides,<sup>5</sup> and hydroxides,<sup>6–8</sup> which are redox-active and able to undergo reversible faradic reactions, are chosen as electrodes or coated onto conductive porous matrix to enhance the electrode performance for high-energy storage capability.

Recently, layered compounds, especially electrochemically active layered double hydroxides (LDH), have drawn increasing

Received: June 30, 2014

Accepted: October 14, 2014

Published: October 14, 2014

attention as electrode materials for high-performance supercapacitors.<sup>9,10</sup> The layered nanostructures prefer to exhibit not only the large specific surface areas but also sufficient interspacing for the intercalation of foreign ions. It has been proved that the doping of metallic ions into single metallic hydroxide structure may help widen the interlayer space and reduce the structure's mechanical stress during charge/discharge processes, therefore leading to obvious increases in its electrochemical capacitances and prohibition in the failure of the electrodes.<sup>11</sup> Nickel–cobalt-based LDH, with its theoretical capacitance  $\approx 3000$  F/g, has been considered as a promising electrode material for pseudosupercapacitors, for both Ni<sup>2+</sup> and Co<sup>2+</sup> are redoxactive in charge/discharge processes.<sup>12</sup> However, such LDH tends to be formed with variable compositions and surface areas under different synthetic routes and shows morphology-dependent electrode performance.<sup>13,14</sup> Furthermore, due to the poor conductivity of Ni/Co LDH, it is often in situ grown on conductive matrix, such as stainless steel sheet,<sup>15</sup> Ni foam,<sup>16,17</sup> TiN nanotubes,<sup>18</sup> zinc–tin oxide (ZTO) nanowires,<sup>19</sup> and NiCo<sub>2</sub>O<sub>4</sub> nanowires (on carbon fiber paper).<sup>20</sup> However, these matrixes could not achieve both high conductivity and large specific area. High-density growth of Ni/Co LDH nanostructure on highly conductive scaffolds with large specific areas is a key to achieving its electrode performance toward theoretical capacitance. For this purpose, carbon nanotubes (CNTs) have been dispersed and employed as matrix to anchor LDH via chemical deposition.<sup>21</sup> However, the wrapping of LDH deposited around individual CNTs or small bundles tends to isolate the intercontacts between adjacent CNTs and therefore inhibits the formation of continuous conductive CNT paths upon electrode fabrication. Additionally, when polymer binder such as Nafion is used, the active area of LDH electrode and its electrochemical performance may be worsened as well. Although the CNT film was tried for this purpose, the small diameters of CNTs and confined porous structure led to the low loading mass of LDH on the film that could be grown on it.<sup>22</sup> It is still a challenge to achieve scalable and high-density growth of Ni/Co LDH nanostructures on CNT scaffolds while keeping the integrity of conductive network for paperlike electrodes with high electrochemical capacitance.

In this research, we developed a simple approach for in situ high-density growth of Ni–Co LDH on conductive CNT buckypaper via precipitation of Co/Ni salts in ammonia solution at room temperature. A freestanding CNT buckypaper with porous structure and high conductivity (thickness  $\approx 70$   $\mu\text{m}$ , square resistance  $< 5$   $\Omega/\square$ ) was used as the matrix. LDH nanoflakes were favorably and densely formed around CNTs in this networked buckypaper. The loading mass of LDH on the CNT network and its chemical composition could be tailored easily by tuning the concentration and relative weight ratio of Ni and Co salts. It was observed that the defective sites were initial nuclei to trigger the growth of LDH nanoflakes, and the latter dense prolongation was more favored around thick CNTs. Furthermore, some of the CNT contacts were well-reserved during the deposition of LDH. As a result, the hierarchical nanostructures could be directly applied for binder-free electrode fabrication. Under optimal composition, the LDH/CNT electrode showed remarkably enhanced performance of LDH nanoflakes with specific capacitance at 2633 F/g under 0.5 A/g, close to theoretical value. Its energy density could be reached at 51 W h/kg with power density kept at 3.3 kW/kg. This research presents a facile approach for in situ

assembling of Ni/Co LDH nanostructures into paper-shaped electrode via room-temperature solution deposition, which may show great potential for high-performance and lightweight energy-storage devices.

## EXPERIMENTAL SECTION

**Materials.** Multiwalled CNTs (MWCNTs) with large diameter of  $\sim 80$  nm were synthesized by floating catalyst chemical vapor deposition (FCCVD) method.<sup>23</sup> The densely packed MWCNT bulks with vertically aligned form were sheared into fluffy “CNT cotton” and purified with high-concentration hydrochloric acid. After that, these CNTs were uniformly dispersed into water with certain dispersant and then vacuum filtrated to prepare a free-standing MWCNT paper as reported formerly.<sup>24</sup> All chemical reagents were of analytical grade and purchased from Sinopharm Chemical Reagent Co., Ltd. (Shanghai, PRC).

**Synthesis.** Ni–Co LDH was grown on CNT paper by a chemical deposition method.<sup>25</sup> Typically, NiCl<sub>2</sub> and CoCl<sub>2</sub> were dissolved in water with a total concentration of 1 M, and a piece of CNT paper was fixed on a glass slide and immersed into this solution. An ammonia (NH<sub>3</sub>·H<sub>2</sub>O) with a concentration of 5% was added dropwise into the solution with intensive mixing, until the pH value of the solution reached 9. Afterward, the solution was kept mixing for 3 h; and finally, the samples were washed by water and ethanol and then dried at room temperature for about 48 h (20 °C). The hydroxide mass on CNT papers was calculated by weighting the mass of CNT paper before and after chemical deposition process.

**Characterization and Tests.** The morphologies of the samples were characterized by scanning electron microscope (SEM, Quanta 400 FEG, FEI, with Apollo 40 SDD X-ray Energy Dispersive Spectrometer (EDS)) and transmission electron microscope (TEM, Tecnai G2 F20 S-Twin, FEI). The crystal structure of the samples was investigated by X-ray powder diffractometer (XRD, D8 Advance, Bruker AXS) and laser micro-Raman spectrometer (LabRam HR 800, Horiba Jobin Yvon). The pore structure of the samples was analyzed by Tristar II 3020 Surface Area Analyzer (Micrometrics). Before measurements, the samples were degassed in vacuum at 200 °C for at least 6 h. The Brunauer–Emmett–Teller (BET) method and the Barrett–Joyner–Halenda (BJH) model were used to test and calculate the specific surface areas and the pore size distributions, respectively.

The electrochemical performance of the samples was studied in a three-electrode test system by using a CHI 660 electrochemical workstation. A platinum wire and a saturated calomel electrode (SCE) were used as the counter electrode and reference electrode, respectively. Six M KOH aqueous solution was used as the electrolyte.

## RESULTS AND DISCUSSION

The as-prepared CNT paper with the size of 20 cm  $\times$  12 cm (length  $\times$  width) was shown by the inset of Supporting Information, Figure S1a. The pristine CNT paper prepared by vacuum filtration method<sup>26,27</sup> has a uniform CNT network structure as shown in Supporting Information, Figure S1a,b. In addition, these CNTs have high crystallization that was confirmed by the clear crystal lattice stripe in the TEM images and Raman spectrum (Supporting Information, Figure S1c,d). The large diameter of these MWCNTs makes them have a low radius-of-curvature surface. These characteristics were beneficial for the growing of nanostructure materials with large loading mass. Figure 1 is a schematic illustration that shows the preparation process and the resulting CNT/Ni–Co LDH nanoflake structure. Figure 2a shows an optical image of the hybrid paper prepared from chemical deposition solution with Ni/Co mole ratio of 3/1. The color of the paper was green because of the deposition of Ni–Co LDH, and the LDH loading mass was calculated to be 233 wt % compared with pristine CNT paper (70 wt % of the hybrid paper, 9.3 mg/cm<sup>2</sup>

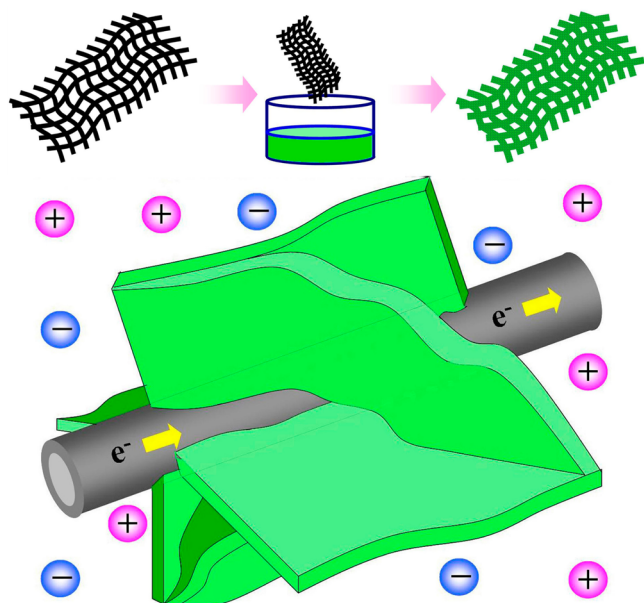


**Figure 1.** Sketch map shows the preparation process and structure of CNT/Ni–Co hydroxide.

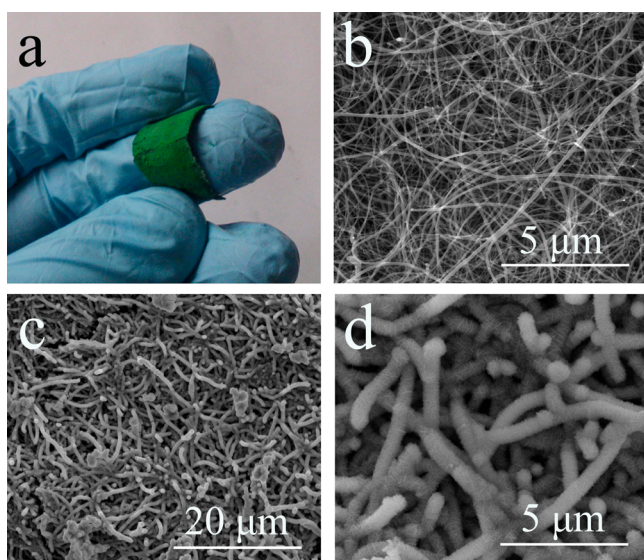


**Figure 2.** Optical image of CNT/ $\text{Co}_{0.4}\text{Ni}_{0.6}(\text{OH})_2$  hybrid paper (a); surface morphology of pristine CNT paper (b); and CNT/ $\text{Co}_{0.4}\text{Ni}_{0.6}(\text{OH})_2$  hybrid paper (c, d).

of LDH on CNT paper). SEM images of this sample are shown in Figure 2c,d. It can be seen that CNTs in the paper were wrapped uniformly by Ni–Co LDH nanoflakes, forming numerous hierarchical structured nanocables. Compared with the pristine CNT paper in Figure 2b, these hierarchical nanocables (Figure 2d) show much larger diameters ( $\sim 500$  nm). Furthermore, there exist many branched nanocables, which indicate that the hydroxide nanoflakes grew not only on the individual CNTs but also in the contact sites between CNTs. This characteristic enables the CNT network in the hybrid paper to be integrated and conductive, which is essential to high-performance electrodes of supercapacitors. Although the hydroxide on CNT paper has a high mass loading, the surface conductivity of the hybrid paper is not too large. Its square resistance is about  $300 \Omega/\square$ , while the pure hydroxide

was close to insulator. The high conductivity was beneficial for enhancing the electrochemical performance of the electrode.

The morphology of CNT/Ni–Co hydroxide nanocable is shown in Figure 3. The hierarchical nanocable coated with large

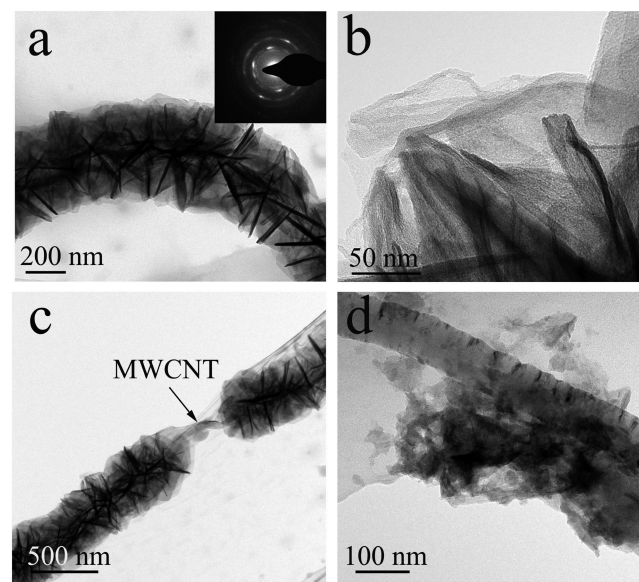


**Figure 3.** TEM images of CNT@ $\text{Co}_{0.4}\text{Ni}_{0.6}(\text{OH})_2$  nanoflake core/shell nanowire in the hybrid paper (a, b); (inset) electron diffraction of LDH nanoflake in the nanowire; discontinuous  $\text{Co}_{0.4}\text{Ni}_{0.6}(\text{OH})_2$  layer coated CNTs (c); and defects on individual CNT (d).

Ni–Co LDH nanoflakes still maintains freestanding as shown in Figure 3a. The selected area electron diffraction of these nanoflakes shows a typical polycrystalline pattern (inset of Figure 3a). It means that these nanoflakes have low crystallinity with abundant defects that endows them with high pseudocapacitive activities when used as supercapacitors electrode. Figure 3b,c shows the nanoflakes are ultrathin with large lateral size (more than 200 nm wide and thinner than 3 nm) compared with the CNT core. These characteristics ensure the nanoflake with large specific area and high loading mass on CNT scaffold.

The growth mechanism of LDH nanoflakes on individual CNTs was investigated by using CNT powder (the raw materials of CNT paper) as the matrix, for the difficult-to-collect CNT paper sample in different stages of the deposition process. However, as CNTs are the same in CNT paper, the morphologies and deposition process of hydroxides on individual CNTs could not be affected. Therefore, a 50 mg CNT powder was first uniformly dispersed into a mixed aqueous solution of 15 mL of  $\text{NiCl}_2$  (1 M) and 5 mL of  $\text{CoCl}_2$  (1 M). As in the above experiment, 25 mL of 5% ammonia aqueous solution could make the pH value of the solution to achieve 9. Here 25 mL of 5% ammonia was slowly added into the solution with strong mixing, and 1 mL of solution sample was taken out after each 5 mL of ammonia aqueous solution was added. It can be seen from Supporting Information, Figure S2a that small LDH nanoplatelets start to form in the surface of individual CNTs after the first 5 mL of ammonia was added. The abundant stripelike cupped structures (shown by the arrow in Figure 3d) on individual CNT surface could be the preferential sites for LDH nanoplatelet to nucleate and grow, and some of these nanoflakes were obviously seen under SEM after the adding of 10 mL of ammonia (Supporting

Information, Figure S2b). Supporting Information, Figure S2c shows that most of the CNTs were covered by vertically aligned LDH nanoflake arrays after 15 mL of ammonia was added. However, there are still some CNTs exposed without whole coverage of LDH nanoflakes as the site shown by arrow in Supporting Information, Figure S2c. The synthesized nanoflakes joined with each other, forming a hierarchical hoop surrounding individual CNTs, and these hoops enable close interface interaction between the nanoflakes and the CNTs. Supporting Information, Figure S2d shows that all of the CNTs were covered by nanoflake arrays after the adding of 20 mL of ammonia. The close contact between the conductive CNT and the electrochemical capacitive LDH nanoflake facilitates rapid electron transfer between them; thus, it is promising in maintaining high electrochemical capacity of the composite structures when large charge–discharge current densities were applied. EDS mapping was used to investigate the element distribution of the nanoflakes, and the results were given in Supporting Information, Figure S3. It can be seen that the two main metallic elements in the nanoflakes, namely, Ni and Co, are uniformly distributed throughout the hierarchical nanowire, which means that the nanoflake is a typical LDH but not the simple mixing of  $\text{Co}(\text{OH})_2$  and  $\text{Ni}(\text{OH})_2$ .

We further studied the influence of matrix on the morphology of LDH nanostructures, and the results are demonstrated in Supporting Information, Figure S4. The nanoflakes directly grown in the solution without other matrices were assembled into random particles (Supporting Information, Figure S4a,b). When small diameter (<10 nm) MWCNTs were used, nanoflowers with a sphere shape were formed along the length direction of CNTs (Supporting Information, Figure S4c,d). These suggest that the diameter of CNTs could be decisive for the uniform coating of LDH nanoflake on individual nanotubes in CNT paper. As shown in Figures 2 and 3, large-diameter MWCNTs with large curvature radius were beneficial for the growth and uniform assembly of LDH nanoflakes. In contrast, when CNTs used with a small diameter that was not much larger than the thickness of LDH nanoflakes, it would be difficult for the vertical growth of LDH. As a result, the LDH nanoflake arrays rearranged into discontinuous nanoflowers. Furthermore, on planelike heterogeneous matrix, such as a nickel foam, the LDH nanoflakes would assemble into large nanoflowers with a stacklike shape, as can be seen in Supporting Information, Figure S4e,f. Supporting Information, Figure S5 is a sketch map that shows the influence of nucleation matrix on the morphologies of LDH nanostructures.

The influence of Ni/Co mole ratio on the morphologies of LDH nanostructures on CNT paper was also investigated. Precursor solutions with four different Ni/Co mole ratios (1/0, 9/1, 1/1, 0/1) were used for comparison, and the results are demonstrated in Supporting Information, Figure S6. Figure 4a shows the relationship between the Ni/Co mole ratio in the precursor solution and the corresponding hydroxide depositing mass and the Ni/Co mole ratio in the as-prepared hydroxide. The precursor solution with pure  $\text{NiCl}_2$  gave birth to large-scale and lath-shaped  $\text{Ni}(\text{OH})_2$  nanoflakes on CNT paper (Supporting Information, Figure S6a) with an ultralarge loading mass of  $\sim 1100\%$  compared with that of pristine CNT paper. These nanoflakes completely coated the surface of CNT paper and covered its porous structure, which was disadvantageous for the diffusion of electrolyte into the electrode and its electrochemical performance. However, when 10% of Co was

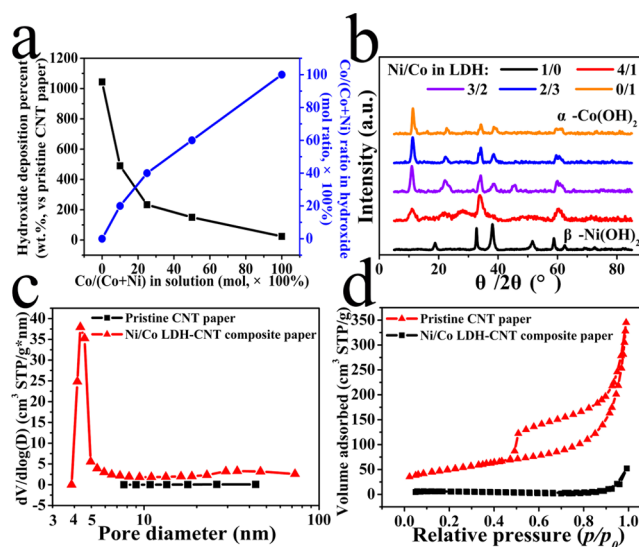


**Figure 4.** Loading mass and chemical components of Ni–Co hydroxide deposited on CNT papers with different chemical deposition solutions (a) and the corresponding XRD patterns (b); adsorption/desorption isotherm curves (c) and corresponding pore-size distribution (d) of pristine CNT paper, and CNT/ $\text{Co}_{0.4}\text{Ni}_{0.6}(\text{OH})_2$  nanoflake hybrid paper.

introduced into precursor solution (Ni/Co mole ratio of 9/1), hydroxide microwires would grow along individual CNTs in the CNT paper as shown in Supporting Information, Figure S6b. EDS result shows that the hydroxide synthesized has a chemical composition of  $\text{Co}_{0.2}\text{Ni}_{0.8}(\text{OH})_2$ . These microwires were composed of ultrathin hydroxide nanoflakes, which could be observed with high-resolution SEM (Supporting Information, Figure S6b). It means that the introduction of Co could reduce the thickness of hydroxide crystals. The specific area of the composite paper was greatly increased, which was beneficial for the utilizing of hydroxide as electrochemical-active materials, although the depositing mass ratio of hydroxide nanoflake to CNT paper was decreased to 500%. When decreasing the Ni/Co mole ratio to 3/1 in the precursor solution, as shown in Figure 2c,d, the size of the LDH nanoflake ( $\text{Co}_{0.4}\text{Ni}_{0.6}(\text{OH})_2$ ) would be suitable for its uniform coating on individual CNTs, and the depositing mass ratio was calculated to be 233% of the pristine CNT paper mass. Further increasing the content of Co to 50%, in solution, the thickness of LDH nanoflake was increased, while the mass ratio was decreased to 150% (Supporting Information, Figure S6c). And the EDS result demonstrates the resulting hydroxide has a chemical composition of  $\text{Co}_{0.6}\text{Ni}_{0.4}(\text{OH})_2$ . Supporting Information, Figure S6d shows that pure  $\text{Co}(\text{OH})_2$  nanoflakes were thicker than Ni/Co LDH and could not form a uniform coating layer on individual CNTs in the CNT paper, resulting in a small loading mass ratio of 25%. The decreased mass loading of hydroxide on CNT paper along with the increase of Co content in the precursor solution was attributed to the preferential deposition of Co-based hydroxide.  $\text{Ni}^{2+}$  ion in aqueous solutions with  $\text{NH}_4^+$  would first assemble into the complex ion  $[\text{Ni}(\text{NH}_3)_x(\text{H}_2\text{O})_{6-x}]^{2+}$  and keep stable for a long time before depositing in the form of hydroxide. However, a  $\text{Co}^{2+}$  ion could be easily deposited as hydroxide in the presence of ammonia, and the slow  $\text{Ni}^{2+}$  deposition could be accelerated by  $\text{Co}^{2+}$  hydroxide to form LDH structure with certain chemical compositions. However, the rapid growth of hydroxide

nanoflakes reduced the dependence of nanoflake nucleation on CNT surface. In other words, the hydroxide grew faster, and few of them chose CNTs as matrix. Instead, most of the hydroxide nanoflakes directly nucleated at the surface of deposited hydroxide particles in the solution with Ni/Co mole ratio smaller than 1/1, and only a small crystal-forming speed proceeded for hydroxide to nucleate and grow using CNT surface as the heterogeneous nucleation center, which finally led to a large mass loading of hydroxide nanoflakes on CNT paper. In addition, the diameter of CNTs should be large enough to match the growth and assembly of thin hydroxide nanoflakes. Therefore, only  $\text{Co}_{0.4}\text{Ni}_{0.6}(\text{OH})_2$  LDH could form a uniform nanoflake coating on large-diameter CNT papers.

The XRD method was used to investigate the crystal structure of Ni–Co hydroxide deposited on CNT paper with different Ni/Co mole ratios. Figure 4b shows that pure Ni hydroxide has a typical  $\beta$ -Ni(OH)<sub>2</sub> diffraction pattern. The main diffraction peaks at 32.7° and 38.1° correspond to lattice planes of (100) and (101), respectively. The introduction of Co into the hydroxide could induce the crystal structure of  $\alpha$ -Ni(OH)<sub>2</sub> and  $\alpha$ -Co(OH)<sub>2</sub>. For example, when the mole ratio of Ni/Co in the precursor solution was changed to 3/1, the resulting Ni–Co hydroxide showed a typical diffraction pattern of  $\alpha$ -phase nickel (cobalt) hydroxide with main diffraction peaks of 11.0° for plane (003) and 33.9° for plane (012). While pure Co in the precursor solution led to the generation of pure  $\alpha$ -Co(OH)<sub>2</sub> hydroxide both on the CNT paper and in the solution,  $\alpha$  phase hydroxides of Ni and Co had a turbostratic-disordered structure with large interlayer distance, which would induce two-electron reaction via an electrochemical conversion between  $\alpha$ -X(OH)<sub>2</sub>/ $\gamma$ -XOOH redox couple (X = Ni or Co), and were expected to have a much higher specific capacitance than their  $\beta$  phase counterparts.<sup>28</sup> Furthermore, Co could stabilize  $\alpha$ -Ni(OH)<sub>2</sub> and prevent it from converting to  $\beta$ -Ni(OH)<sub>2</sub>, which can enhance the cyclic performance of the LDH nanoflakes.

The introduction of Ni/Co hydroxide nanoflakes on CNT paper greatly increased the specific surface area of the composite paper. Figure 4c shows the N<sub>2</sub>-adsorption/desorption isotherm curves of pristine CNT paper and CNT/Co<sub>0.4</sub>Ni<sub>0.6</sub>(OH)<sub>2</sub> nanoflakes hybrid paper. It shows that the pristine CNT paper has a small specific surface area of 14.1 m<sup>2</sup>/g, while the composite paper has a typical IV isotherm with H3-type hysteresis loops (P/P<sub>0</sub> > 0.4), indicating the presence of mesopores; the resulting specific surface area was calculated to be 177.4 m<sup>2</sup>/g, much higher than that of pristine CNT paper. The great increase in surface area was attributed to the hierarchical nanostructure formed by hydroxide nanoflakes on CNTs, with most of the pore diameters demonstrated to be in the range of 4–5 nm (Figure 4d). It is known that electrode materials with large surface area could enlarge the contact of the electrode and the electrolyte, and thus benefit the utilizing efficiency of electrochemical active materials. Therefore, CNT/Co<sub>0.4</sub>Ni<sub>0.6</sub>(OH)<sub>2</sub> nanoflake hybrid paper was promising for the application of supercapacitors.

The electrochemical performance of the hydroxide-wrapped CNT paper was demonstrated in Figure 5. Figure 5a shows the cyclic voltammogram (CV) curves of hybrid paper electrodes with different hydroxides in 6 M KOH solution at a scan rate of 5 mV/s. Each of the five curves shows a pair of redox peaks, corresponding to the reversible redox state of X<sup>2+</sup>/X<sup>3+</sup> (X = Ni and Co). The largest redox current density was obtained from CNT/Co<sub>0.4</sub>Ni<sub>0.6</sub>(OH)<sub>2</sub> nanoflake hybrid paper with the ratio of

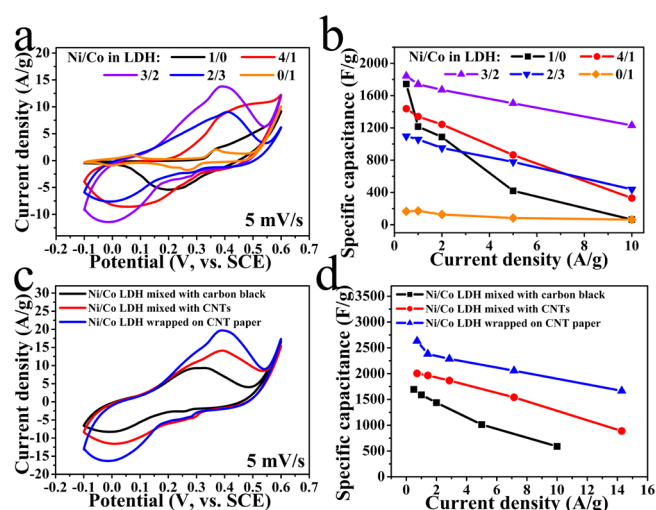


**Figure 5.** CV curves (5 mV/s) (a) and rate performance (b) of CNT/Ni–Co hydroxide hybrid paper with different chemical components of hydroxide; CV curves (c) and rate performance (d) of Co<sub>0.4</sub>Ni<sub>0.6</sub>(OH)<sub>2</sub> composites with different electrode structures.

the anodic and cathodic peak current of  $\sim 1.0$ . This indicates a reversible faradic redox reaction of this sample during the CV test, and it plays the key role in contributing to the pseudocapacitance. Figure 5b shows the specific capacitances of the five samples calculated from charge/discharge curves at different current densities. It reveals that CNT paper wrapped by pure  $\beta$ -Ni(OH)<sub>2</sub> has a large specific capacitance of 1744 F/g at the small current density of 0.5 A/g. However, its rate performance is poor, as specific capacitance of only 64 F/g is maintained when the current density is increased to 10 A/g. This could be attributed to the ultralarge loading mass of hydroxide that formed a compact structure on CNT paper. This kind of surface hindered the diffusion of electrolyte ion into the composite paper; thus, the electrode was easily polarized at large current densities, and the specific capacitances were greatly reduced. This phenomenon could be meliorated by increasing Co content in the precursor solution, resulting in a porous surface with large specific area to facilitate electrolyte ion diffusion. However, this would reduce the hydroxide loading mass on CNT paper (Figure 4a) and decrease the specific capacitance of the composite paper at small current densities. As a result, the CNT/Co<sub>0.4</sub>Ni<sub>0.6</sub>(OH)<sub>2</sub> nanoflake hybrid paper balanced between the rate performance and the specific capacitance among the five specimens. Its charge/discharge curves at different current densities are shown in Supporting Information, Figure S7a. As a typical example, at the current density of 5 A/g, this trend was well-reflected by their specific capacitance values (Figure 5b and Supporting Information, Figure S7b), which are 420, 864, 1504, 778, and 83 F/g when the content of Co in the precursor solution was increased accordingly.

The hierarchical structured nanocable paper with intact conductive CNT network and large loading mass of hydroxide-active materials was far superior to commercial electrode structure (powder with polymer binder). A comparison is given in Figure 5c,d. Here, two other electrodes were used to compare with CNT/Co<sub>0.4</sub>Ni<sub>0.6</sub>(OH)<sub>2</sub> nanoflake hybrid paper. One is pure Co<sub>0.4</sub>Ni<sub>0.6</sub>(OH)<sub>2</sub> nanoflowers prepared in the precursors without matrix, the other is Co<sub>0.4</sub>Ni<sub>0.6</sub>(OH)<sub>2</sub> nanoflowers mixed with CNT powder as is a common structure

of a commercial supercapacitor electrode (CNT content of 30 wt %, the same as the hybrid paper). The two electrodes were prepared by the method of commercialized electrode preparation. Concretely, the mass ratio of LDH and polymer binder (poly(tetrafluoroethylene)) was 85/5. The mixed powder was painted onto Ni foam as a working electrode for the electrochemical test. In Figure 5c,d, the mass used for calculating the electrochemical performance is based on the hydroxide in the composite electrode. The results show that the introduction of CNTs as conductive fillers effectively improved the redox peak current densities of the hydroxide (Figure 5c). Besides, the core/shell structured nanocable paper has a larger redox peak current density than that of the other two samples, indicating the best electrochemical performance. The specific capacitances of hydroxide in this sample calculated from charge/discharge curves at different current densities were larger than those of other two samples, which also indicates a good rate performance (Figure 5d). The hydroxide nanoflakes in this electrode have a high specific capacitance of 2633 F/g at a low current density of 0.7 A/g and maintains at 1666 F/g at a large current density of 14 A/g, while the pure hydroxide and the hydroxide mixed with 30 wt % CNTs electrodes could only reach to 591 F/g at 10 A/g and 889 F/g at 14 A/g, respectively.

Ragone plots of the three kinds of hydroxides calculated from charge/discharge curves at different current densities are shown in Figure 6a. The energy density of the hydroxide in the

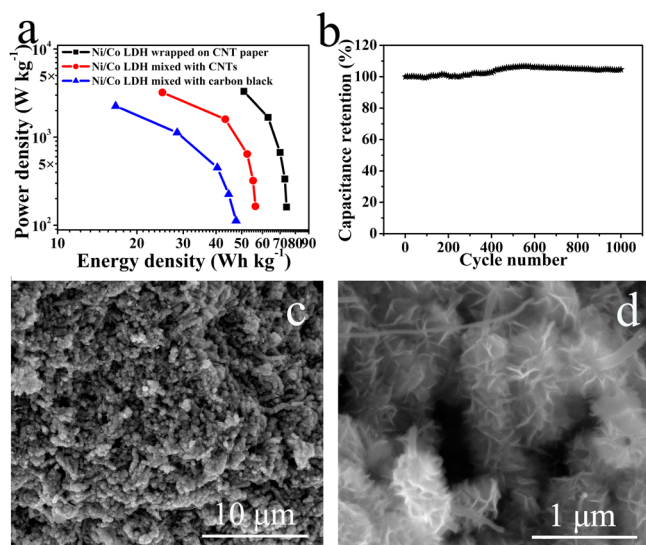


**Figure 6.** Ragone plots of  $\text{Co}_{0.4}\text{Ni}_{0.6}(\text{OH})_2$  composite with different electrode structures (a); cyclic performance of  $\text{CNT}/\text{Co}_{0.4}\text{Ni}_{0.6}(\text{OH})_2$  nanoflake hybrid paper at a current density of 2 A/g (b); and the morphologies of the hybrid paper after cyclic performance tests (c, d).

composite paper could achieve 74.0 W h/kg with a power density of 0.16 kW/kg, which maintains at 51.0 W h/kg at the power density of 3.30 kW/kg. While the pure hydroxide powder electrode maintains an energy density of as low as 16.6 W h/kg when its power density increases to 2.25 kW/kg.

The electrochemical performance enhancement of hybrid paper could be attributed to the porous hydroxide structure, the intact conductive CNT network, and the close contact between them. As a supercapacitor electrode, a porous structure with large surface area was essential to the facile diffusion of electrolyte into the inner part of the electrode, which can lead to the maximum utilizing of electrochemical active materials of

the electrode. Comparing with Ni/Co oxide nanostructures such as nickel oxide,<sup>29,30</sup> cobalt oxide,<sup>31,32</sup> and  $\text{NiCo}_2\text{O}_4$ ,<sup>33,34</sup> the LDH has better compatibility with aqueous electrolytes for the abundant hydration groups on their surface. Thus,  $\text{CNT}/\text{Co}_{0.4}\text{Ni}_{0.6}(\text{OH})_2$  nanoflake hybrid paper showed better electrochemical performance than  $\text{CNT}/\text{Ni}$  (Co) oxide composites. Commercial electrode for supercapacitors was usually prepared by mechanically mixing the electrochemical active materials (active carbon or metallic oxide/hydroxide) and the conductive fillers (CNTs, graphene, or conductive carbon black). This method could not achieve uniform dispersion of conductive fillers in submicrometer scale, and thus, was not able to form an efficient conductive network in the electrode. In addition, the active materials were difficult to form effective contact with the conductive fillers in this case. These characteristics greatly restricted the efficient utilizing of electrochemical active materials, and limited the electrochemical performance of the electrode. The chemical deposition synthesis of  $\text{CNT}/\text{Co}_{0.4}\text{Ni}_{0.6}(\text{OH})_2$  hybrid paper could achieve both the integrated CNT conductive network and the good contact between the CNTs and the LDH nanoflakes. This structure was beneficial for electron transport in the electrode and largely improved the electrochemical performance of LDH nanoflakes in the hybrid paper, especially at large current densities. The close contact structure between the CNTs and the LDH nanoflakes was stable and not easily damaged, as demonstrated by Figure 6b–d. The specific capacitance of  $\text{CNT}/\text{Co}_{0.4}\text{Ni}_{0.6}(\text{OH})_2$  nanoflake hybrid paper reaches to 107% of its initial value after 500 cycles of charge/discharge at a current density of 2 A/g (Figure 6b). The slight increase of capacitance could be attributed to the gradual increase of the electrolyte diffusing into the porous electrode and the conversion of  $\text{Ni}_x\text{Co}_{2-x}(\text{OH})_2$  to  $\text{Ni}_{x/2}\text{Co}_{1-x/2}\text{OOH}$ .<sup>35</sup> Furthermore, the capacitance of this sample could be slightly decreased after 600 cycles. Figure 6c,d shows the morphologies of this sample after the cyclic test. It can be seen that the hierarchical nanocable structures are well-maintained, which indicates the volume expanding/shrinking resulted from the charge/discharge redox reaction of Ni/Co LDH could not lead to the detachment of hydroxide nanoflake from CNT skeletons.

## CONCLUSIONS

In summary, a  $\text{CNT}@\text{Ni-Co}$  LDH nanoflake hierarchical nanocable paper was prepared by a facile chemical deposition method. Ultrathin and large-scale Ni–Co LDH nanoflakes were grown orderly on the surface of individual CNTs in a freestanding CNT paper. The resulting  $\text{CNT}/\text{LDH}$  hybrid paper with intact conductive network had a large specific surface area and demonstrated excellent electrochemical performance compared with commercialized electrodes. The morphology and loading mass of LDH on CNT paper were controlled by modifying the component of the precursor solution. The formation of these hierarchical nanocables was attributed to the rough surface of individual CNTs and the layered structure of Ni–Co LDH. The composite paper serves as a promising candidate for the electrodes of advanced devices for energy storage.

## ASSOCIATED CONTENT

### Supporting Information

Additional characterization data; SEM images of pristine CNT paper, LDH growth process, LDH grown on different substrates, and Ni/Co hydroxides with different chemical

compositions on CNT paper; EDX mapping; and charge/discharge curves. This material is available free of charge via the Internet at <http://pubs.acs.org>.

## AUTHOR INFORMATION

### Corresponding Authors

\*E-mail: mhchen2008@sinano.ac.cn. (M.C)

\*E-mail: qwli2007@sinano.ac.cn. (Q.L)

### Notes

The authors declare no competing financial interest.

## ACKNOWLEDGMENTS

This work was supported by the National Science Foundation of China (No. 21203238), the National Basic Research Program (No. 2011CB932600-G), and Knowledge Innovation Program (KJJCX2.YW.M12) of the Chinese Academy of Sciences.

## REFERENCES

- (1) Dunn, B.; Kamath, H.; Tarascon, J.-M. Electrical Energy Storage for the Grid: A Battery of Choices. *Science* **2011**, *334*, 928–935.
- (2) Simon, P.; Gogotsi, Y. Materials for Electrochemical Capacitors. *Nat. Mater.* **2008**, *7*, 845–854.
- (3) Ghosh, A.; Lee, Y. H. Carbon-Based Electrochemical Capacitors. *ChemSusChem* **2012**, *5*, 480–499.
- (4) Wang, K.; Wu, H.; Meng, Y.; Wei, Z. Conducting Polymer Nanowire Arrays for High Performance Supercapacitors. *Small* **2014**, *10*, 14–31.
- (5) Jiang, J.; Li, Y.; Liu, J.; Huang, X.; Yuan, C.; Lou, X. W. D. Recent Advances in Metal Oxide-based Electrode Architecture Design for Electrochemical Energy Storage. *Adv. Mater.* **2012**, *24*, 5166–5180.
- (6) Ji, J.; Zhang, L. L.; Ji, H.; Li, Y.; Zhao, X.; Bai, X.; Fan, X.; Zhang, F.; Ruoff, R. S. Nanoporous Ni(OH)<sub>2</sub> Thin Film on 3D Ultrathin-Graphite Foam for Asymmetric Supercapacitor. *ACS Nano* **2013**, *7*, 6237–6243.
- (7) Hercule, K. M.; Wei, Q.; Khan, A. M.; Zhao, Y.; Tian, X.; Mai, L. Synergistic Effect of Hierarchical Nanostructured MoO<sub>2</sub>/Co(OH)<sub>2</sub> with Largely Enhanced Pseudocapacitor Cyclability. *Nano Lett.* **2013**, *13*, 5685–5691.
- (8) Xia, X.; Tu, J.; Zhang, Y.; Chen, J.; Wang, X.; Gu, C.; Guan, C.; Luo, J.; Fan, H. J. Porous Hydroxide Nanosheets on Preformed Nanowires by Electrodeposition: Branched Nanoarrays for Electrochemical Energy Storage. *Chem. Mater.* **2012**, *24*, 3793–3799.
- (9) Shao, M.; Ning, F.; Zhao, Y.; Zhao, J.; Wei, M.; Evans, D. G.; Duan, X. Core–Shell Layered Double Hydroxide Microspheres with Tunable Interior Architecture for Supercapacitors. *Chem. Mater.* **2012**, *24*, 1192–1197.
- (10) Han, J.; Dou, Y.; Zhao, J.; Wei, M.; Evans, D. G.; Duan, X. Flexible CoAl LDH@PEDOT Core/Shell Nanoplatelet Array for High-Performance Energy Storage. *Small* **2013**, *9*, 98–106.
- (11) Wang, Q.; O'Hare, D. Recent Advances in the Synthesis and Application of Layered Double Hydroxide (LDH) Nanosheets. *Chem. Rev.* **2012**, *112*, 4124–4155.
- (12) Yan, T.; Zhu, H.; Li, R.; Li, Z.; Liu, J.; Wang, G.; Gu, Z. Microwave Synthesis of Nickel/Cobalt Double Hydroxide Ultrathin Flowerclusters with Three-Dimensional Structures for High-Performance Supercapacitors. *Electrochim. Acta* **2013**, *111*, 71–79.
- (13) Liu, X.; Ma, R.; Bando, Y.; Sasaki, T. A General Strategy to Layered Transition-Metal Hydroxide Nanocones: Tuning the Composition for High Electrochemical Performance. *Adv. Mater.* **2012**, *24*, 2148–2153.
- (14) Yan, T.; Li, Z.; Li, R.; Ning, Q.; Kong, H.; Niu, Y.; Liu, J. Nickel–Cobalt Double Hydroxides Microspheres with Hollow Interior and Hedgehog-Like Exterior Structures for Supercapacitors. *J. Mater. Chem.* **2012**, *22*, 23587–23592.
- (15) Salunkhe, R. R.; Jang, K.; Lee, S.-W.; Ahn, H. Aligned Nickel–Cobalt Hydroxide Nanorod Arrays for Electrochemical Pseudocapacitor Applications. *RSC Adv.* **2012**, *2*, 3190–3193.
- (16) Liu, X.; Huang, J.; Wei, X.; Yuan, C.; Liu, T.; Cao, D.; Yin, J.; Wang, G. Preparation and Electrochemical Performances of Nanostructured Co<sub>x</sub>Ni<sub>1-x</sub>(OH)<sub>2</sub> Composites for Supercapacitors. *J. Power Sources* **2013**, *240*, 338–343.
- (17) Chen, H.; Hu, L.; Chen, M.; Yan, Y.; Wu, L. Nickel–Cobalt Layered Double Hydroxide Nanosheets for High-performance Supercapacitor Electrode Materials. *Adv. Funct. Mater.* **2014**, *24*, 934–942.
- (18) Shang, C.; Dong, S.; Wang, S.; Xiao, D.; Han, P.; Wang, X.; Gu, L.; Cui, G. Coaxial Ni<sub>x</sub>Co<sub>2-x</sub>(OH)<sub>2</sub>/TiN Nanotube Arrays as Supercapacitor Electrodes. *ACS Nano* **2013**, *7*, 5430–5436.
- (19) Wang, X.; Sumboja, A.; Lin, M.; Yan, J.; Lee, P. S. Enhancing Electrochemical Reaction Sites in Nickel–Cobalt Layered Double Hydroxides on Zinc Tin Oxide Nanowires: a Hybrid Material for an Asymmetric Supercapacitor Device. *Nanoscale* **2012**, *4*, 7266–7272.
- (20) Huang, L.; Chen, D.; Ding, Y.; Feng, S.; Wang, Z. L.; Liu, M. Nickel–Cobalt Hydroxide Nanosheets Coated on NiCo<sub>2</sub>O<sub>4</sub> Nanowires Grown on Carbon Fiber Paper for High-Performance Pseudocapacitors. *Nano Lett.* **2013**, *13*, 3135–3139.
- (21) Zhao, J.; Chen, J.; Xu, S.; Shao, M.; Zhang, Q.; Wei, F.; Ma, J.; Wei, M.; Evans, D. G.; Duan, X. Hierarchical NiMn Layered Double Hydroxide/Carbon Nanotubes Architecture with Superb Energy Density for Flexible Supercapacitors. *Adv. Funct. Mater.* **2014**, *24*, 2938–2946.
- (22) Salunkhe, R. R.; Jang, K.; Lee, S.-W.; Yu, S.; Ahn, H. Binary Metal Hydroxide Nanorods and Multi-Walled Carbon Nanotube Composites for Electrochemical Energy Storage Applications. *J. Mater. Chem.* **2012**, *22*, 21630–21635.
- (23) Andrews, R.; Jacques, D.; Rao, A. M.; Derbyshire, F.; Qian, D.; Fan, X.; Dickey, E. C.; Chen, J. Continuous Production of Aligned Carbon Nanotubes: A Step Closer to Commercial Realization. *Chem. Phys. Lett.* **1999**, *303*, 467–474.
- (24) Chen, H.; Chen, M.; Di, J.; Xu, G.; Li, H.; Li, Q. Architecting Three-Dimensional Networks in Carbon Nanotube Buckypapers for Thermal Interface Materials. *J. Phys. Chem. C* **2012**, *116*, 3903–3909.
- (25) Lang, J. W.; Kong, L. B.; Liu, M.; Luo, Y. C.; Kang, L. Co<sub>0.56</sub>Ni<sub>0.44</sub> Oxide Nanoflake Materials and Activated Carbon for Asymmetric Supercapacitor. *J. Electrochem. Soc.* **2010**, *157*, A1341–A1346.
- (26) Jin, Y.; Chen, H.; Chen, M.; Liu, N.; Li, Q. Graphene-Patched CNT/MnO<sub>2</sub> Nanocomposite Papers for the Electrode of High-Performance Flexible Asymmetric Supercapacitors. *ACS Appl. Mater. Interfaces* **2013**, *5*, 3408–3416.
- (27) Chen, H.; Di, J.; Jin, Y.; Chen, M.; Tian, J.; Li, Q. Active Carbon Wrapped Carbon Nanotube Buckypaper for the Electrode of Electrochemical Supercapacitors. *J. Power Sources* **2013**, *237*, 325–331.
- (28) Gao, X.-P.; Yang, H.-X. Multi-Electron Reaction Materials for High Energy Density Batteries. *Energy Environ. Sci.* **2010**, *3*, 174–189.
- (29) Gund, G. S.; Dubal, D. P.; Shinde, S. S.; Lokhande, C. D. Architected Morphologies of Chemically Prepared NiO/MWCNTs Nanohybrid Thin Films for High Performance Supercapacitors. *ACS Appl. Mater. Interfaces* **2014**, *6*, 3176–3188.
- (30) Wu, M. S.; Zheng, Y. R.; Lin, G. W. Three-Dimensional Carbon Nanotube Networks with a Supported Nickel Oxide Nanonet for High-Performance Supercapacitors. *Chem. Commun.* **2014**, *50*, 8246–8248.
- (31) Liu, S.; Zuo, M. Facile Synthesis of Cobalt Oxide Uniformly Coated on Multi-Wall Carbon Nanotubes for Supercapacitors. *Adv. Mater. Res.* **2011**, 1148–1152.
- (32) Lang, J.; Yan, X.; Xue, Q. Facile Preparation and Electrochemical Characterization of Cobalt Oxide/Multi-Walled Carbon Nanotube Composites for Supercapacitors. *J. Power Sources* **2011**, *196* (18), 7841–7846.
- (33) Liu, W.; Lu, C.; Liang, K.; Tay, B. K. A Three Dimensional Vertically Aligned Multiwall Carbon Nanotube/NiCo<sub>2</sub>O<sub>4</sub> Core/Shell Structure for Novel High-Performance Supercapacitors. *J. Mater. Chem. A* **2014**, *2*, 5100–5107.

(34) Zhang, G.; Lou, X. W. D. Controlled Growth of NiCo<sub>2</sub>O<sub>4</sub> Nanorods and Ultrathin Nanosheets on Carbon Nanofibers for High-performance Supercapacitors. *Sci. Rep.* **2013**, *3*, 1470.

(35) Zhang, J.; Fu, J.; Zhang, J.; Ma, H.; He, Y.; Li, F.; Xie, E.; Xue, D.; Zhang, H.; Peng, Y. Co@Co<sub>3</sub>O<sub>4</sub> Core–Shell Three-Dimensional Nano-Network for High-Performance Electrochemical Energy Storage. *Small* **2014**, *10*, 2618–2624.